A theoretical study on the anomalous pressure dependence of the transport properties of ionic liquids: Comparison among lithium bromide, silica, and water

T. Yamaguchi,[a] A. Nagao, T. Matsuoka, and S. Koda
Department of Molecular Design and Engineering, Graduate School of Engineering, Nagoya University, Chikusa, Nagoya, Aichi 464-8603, Japan

(Received 18 June 2003; accepted 5 September 2003)

The transport coefficients of three ionic liquids, lithium bromide (LiBr), rubidium bromide (RbBr), and molten silica (SiO_2) are calculated by the mixture mode-coupling theory. The static partial structure factors required are obtained from the interionic interaction potential by the Ornstein–Zernike/hypernetted-chain integral equation. The anomalous pressure dependence of the transport properties, the increase in the molar ionic conductivity of LiBr and the fluidity of SiO_2 in the low-pressure region, is reproduced qualitatively well by our theoretical calculation. The calculated results are analyzed in the similar way as that for water performed by Yamaguchi *et al.* [T. Yamaguchi, S.-H. Chong, and F. Hirata, J. Chem. Phys. **119**, 1021 (2003)], and we found that the friction on the electric current caused by the coupling between the charge- and number-density modes is effective to the increase of the transport coefficient with pressure, as is the case of water. Comparing the results for LiBr and RbBr, the contribution of the electrostatic friction is smaller for RbBr, which leads to the normal pressure dependence of its molar ionic conductivity. The negative values of the Nernst–Einstein deviation parameter for the ionic conductivity of LiBr and SiO_2 reported by previous MD simulations are also explained consistently. Furthermore, it is shown that the mechanism for the anomalous pressure dependence of the fluidity of molten SiO_2 demonstrated in this work is consistent with a conventional picture that the five-coordinated silicon atom is important to enhance the ionic mobility. © *2003 American Institute of Physics.*
[DOI: 10.1063/1.1622652]

I. INTRODUCTION

The molecular mobilities of most liquids are decreasing functions of pressure. It indicates that the molecules diffuse less easily at more densely packed condition, which is consistent with our everyday experience. However, there are some liquids whose molecular mobility is enhanced by compression, and its microscopic mechanism has been under debate for many years.

The most famous example of such a liquid is water.[1–4] Due to its chemical and biological importance, the equilibrium and transport properties of water have been a target of high-pressure science from the beginning of the last century. Owing to the accumulation of the experimental works, it has been revealed that the molecular mobilities of liquid water, as appear in the shear viscosity, dielectric relaxation, self-diffusion, and single-particle reorientational relaxation, are increasing functions of pressure in the low-temperature, low-pressure region. As is the case of other anomalous properties of water, this pressure dependence of the molecular mobility of water has been ascribed to its tetrahedral hydrogen-bonding network structure.[1–3]

Molten silica (SiO_2) is another liquid that shows anomalous pressure dependence of the transport coefficients. The properties of molten silica and related compounds under high pressure are quite important in geophysics. Although the transport coefficients of neat molten silica have not been reported to our best knowledge, the shear viscosities of related compounds are extensively measured in the high-temperature, high-pressure region mainly by Kushiro *et al.*[5–9] They found that the shear viscosities of many kinds of magma decrease significantly with pressure, which had a great impact on both geophysics and material science. They also measured the self-diffusion coefficients of oxygen atoms of these compounds, and showed that the diffusivity of the oxygen atom is also enhanced by the compression.[10] Stimulated by these experimental findings, there have been many theoretical and computer simulation studies on the anomalous pressure dependence of the transport coefficients of molten SiO_2, and these anomalies are now considered to be due to the pressure-induced breakdown of the tetrahedral network structure,[11–15] just as the anomalous pressure dependence of the dynamic properties of water is ascribed to the breakdown of the tetrahedral hydrogen-bonding network structure.

A less famous example of the anomalous pressure dependence of the transport coefficient is that of the molar ionic conductivity of molten LiBr. Cleaver *et al.* measured the ionic conductivity of various molten alkali halides, and found that the molar conductivities of lithium halides are increasing functions of pressure in the low-pressure region.[16] Tödheide *et al.* studied the pressure dependence of the molar

[a]Electronic mail: tyama@nuce.nagoya-u.ac.jp

conductivity of molten LiBr in detail, and reported that the pressure dependence of the molar conductivity has a maximum value.[17] These experimental facts indicate that the ionic mobilities of molten LiBr is enhanced by compression, as is the case of water and silica. However, the anomaly in the pressure dependence of the molar conductivity of molten LiBr has been discussed in different ways from the corresponding properties of water and silica, since the molten LiBr does not have a tetrahedral network structure as water and silica. For example, Tödheide considers that the electronic polarizability is responsible for the anomalous pressure dependence.[17] On the other hand, Okada *et al.* showed by their molecular dynamics (MD) simulation, using the rigid ion model, that the pressure dependence of the self-exchange velocity of molten LiBr is in harmony with that of the molar conductivity, although they did not evaluate the conductivity explicitly.[18] Very recently, we reported that the pressure dependence of the molar conductivity of LiBr is reproduced qualitatively by the mode-coupling theory (MCT) with the same model.[19]

In a recent work, Yamaguchi *et al.* calculated the dynamic properties of water at various densities and pressures using the generalized Langevin/modified mode-coupling theory devised for molecular liquids described by the interaction-site model.[4] The anomalous pressure dependence of various dynamic properties is reproduced qualitatively well, although the quantitative agreement is not so good. Furthermore, they analyzed their theoretical calculation in detail, and found that the interatomic strong Coulombic interaction can be a reason for the anomalous pressure dependence of dynamic properties. Owing to the decrease in the number-density fluctuation in the low-wave-number region with increasing pressure, the Coulombic coupling between the low-wave-number charge-density fluctuation and hydrodynamic dielectric mode is reduced. They also performed similar analyses on other polar liquids in order to clarify the specificity of water. They found that the effect of Coulombic interaction is hindered by that of repulsive collisions in the case of typical polar liquids as acetonitrile. However, they also demonstrated by both the MCT calculation and MD simulation that the dynamic properties of a model diatomic polar liquid can show the anomalous pressure dependence even if it does not have any kind of tetrahedral hydrogen-bonding network structure.

Ionic liquids are liquids composed of charged particles, so that the intermolecular Coulombic interaction has strong influence on both the equilibrium and dynamic properties. Since the anomalous dynamic properties of water above can be derived from the strong intermolecular Coulombic interaction in general, there is a possibility that the anomalous pressure dependence of the transport coefficients of both molten LiBr and silica melt is explained in the similar way as that of water. Recently, Wilke *et al.* performed a mode-coupling calculation on the ideal glass transition of the symmetric model ionic liquid.[20] They found that the density dependence of the ideal glass transition temperature shows a re-entrant behavior, that is, a vitreous state becomes ergodic by applying the pressure. Although they did not demonstrate explicitly, it indicates that the transport coefficients of the model liquid show the anomalous pressure dependence of mobilities as LiBr, silica, and water, and their calculation supports our idea that the pressure-induced enhancement of the molecular mobility of liquids stems from the general properties of the intermolecular Coulombic interaction.

In this work, we perform mode-coupling calculation of above ionic liquids, LiBr and SiO_2, in order to clarify how the intermolecular interactions and the changes in the liquid structures lead to the pressure-induced enhancement of the molecular mobility. The equilibrium structure required in the MCT calculation is obtained by the statistical integral equation theory as is the case of the corresponding calculation on water.[4] A similar calculation on RbBr, which does not indicate the anomaly in the pressure dependence of the transport coefficients, is also performed for comparison with that of LiBr. The modified mode-coupling theory for molecular liquids employed by Yamaguchi *et al.* is based on the interaction-site model,[4] and the site density is the dynamic variable explicitly considered there. One can therefore translate the analysis of the MCT calculation on water into that on ionic liquids easily, which we consider is a merit of the interaction-site based theory of the dynamics of molecular liquids, as opposed to that based on the spherical harmonics expansion.

II. PREVIOUS MODE-COUPLING ANALYSIS OF THE PRESSURE-INDUCED ENHANCEMENT OF MOLECULAR MOBILITY OF WATER, AND ITS IMPLICATION TO IONIC LIQUIDS

Consider a liquid composed of interaction sites α, γ,.... Here, the greek indices $(\alpha,\gamma,...)$ refer to the species, and i, j,... will be used for the individual sites. At present, it does not matter whether interaction sites are connected by chemical bonds (polar liquids) or not (molten salts). The mass and charge of the site α are denoted as m_α and z_α, respectively.

In the mode-coupling analysis of the anomalous pressure dependence of the molecular mobility of water performed by Yamaguchi *et al.*,[4] the electrostatic friction on the charge-density mode, $\Sigma_\alpha z_\alpha \rho_\alpha(\mathbf{k})$ in the low-wave-number region plays an essential role, where $\rho_\alpha(\mathbf{k})$ represents the number-density mode of site α in the reciprocal space. The charge-density mode in the low-wave-number limit corresponds to the collective dipolar reorientation (dielectric relaxation) in the case of polar molecular liquids, whereas it does to the electric current in the case of ionic liquids.

We will discuss hereafter on two anomalous properties of the dynamics of ionic liquids, the pressure-induced enhancement of the mobility and the negative Nernst–Einstein deviation parameter, in terms of the short-time behavior of the electrostatic friction, as was done for water in Ref. 4. The frictional force other than the electrostatic ones are working in reality, however, and the short-time behavior of the memory function may not be related directly to the time-integrated transport properties. It is therefore required to treat the dynamics of ionic liquids fully on the microscopic level before extracting the effect of electrostatic friction, which we are going to do in this work. As will be shown in Sec. V A, the contribution from the low-wave-number region ($q < 1.5\,\text{Å}^{-1}$) is mainly responsible to the anomalous pressure

dependence of the ionic conductivity, and the short-time behavior is reflected in the zero-frequency character in a rather straightforward way in the case of LiBr, consistent with the picture presented below. In Sec. V C, the electrostatic friction is also shown responsible for the negative Nernst–Einstein deviation parameter. In the case of silica, the presence of the first-sharp-diffraction-peak around 2 Å^{-1} may require a modification of the picture, which will be discussed in Sec. V D.

A. Anomalous pressure dependence

According to the idea based on the fluctuation–dissipation theorem,[21–23] the friction kernel on the charge-density mode in the low-wavelength limit is proportional to the time correlation function of the random force acting on the mode as

$$\zeta(t)=\frac{1}{V}\left\langle\left\{\sum_{\alpha} z_{\alpha}\sum_{i\in\alpha}\mathbf{f}_i(t=0)\right\}\cdot\left\{\sum_{\alpha} z_{\alpha}\sum_{i\in\alpha}\mathbf{f}_i(t)\right\}\right\rangle, \tag{1}$$

where $\mathbf{f}_i(t)$ is the random force acting on the site i.

When the interaction potential between sites, denoted as $\tilde{u}_{\alpha\gamma}(k)$ in the reciprocal space, is pairwise additive and isotropic, the force on the site current is given by

$$\sum_{i\in\alpha}\mathbf{f}_i=\sum_{\mathbf{k}}\sum_{\gamma} i\mathbf{k}\tilde{u}_{\alpha\gamma}(\mathbf{k})\rho_{\alpha}(\mathbf{k})\rho_{\gamma}(-\mathbf{k}). \tag{2}$$

Here the random force is replaced by force and the wave vector is treated as a discrete variable.

By substituting Eq. (2) into Eq. (1), $\zeta(t)$ is described as

$$\zeta(t)\simeq Vk^2\sum_{\mathbf{k}}\sum_{\alpha\gamma\mu\nu} z_{\alpha}z_{\gamma}[\tilde{u}_{\alpha\mu}(\mathbf{k})F^{\mu\nu}(k,t)\tilde{u}_{\nu\gamma}(\mathbf{k})F^{\alpha\gamma}(k,t) - \tilde{u}_{\alpha\mu}(\mathbf{k})F^{\mu\gamma}(k,t)F^{\alpha\nu}(k,t)\tilde{u}_{\nu\gamma}(\mathbf{k})], \tag{3}$$

where we used the factorization approximation involving four density fluctuations as is the case of the mode-coupling theory, and $F^{\alpha\gamma}(k,t)$ is the site–site dynamic structure factor given by

$$F^{\alpha\gamma}(k,t)=\frac{1}{V}\langle\rho_{\alpha}^{*}(\mathbf{k},0)\rho_{\gamma}(\mathbf{k},t)\rangle, \tag{4}$$

where V stands for the volume of the system. It should be noted that the normalization factor, V, is different from other literatures. By replacing the bare interaction potential, $\tilde{u}_{\alpha\gamma}(\mathbf{k})$, with the effective one described by the direct correlation function as $-k_BTc^{\alpha\gamma}(k)$, one can obtain the expression of the mode-coupling theory.[20]

Here we consider the effect of the interatomic Coulombic interaction, so that the interaction potential $\tilde{u}_{\alpha\gamma}(k)$ is replaced by its Coulombic part as

$$\tilde{u}_{\alpha\gamma}(k)\rightarrow\frac{4\pi z_{\alpha}z_{\gamma}}{k^2}. \tag{5}$$

Substituting Eq. (5) into Eq. (3), the Coulombic contribution of $\zeta(t)$ is given by

$$\zeta_{\text{Coulomb}}(t)\propto\sum_{\mathbf{k}}\left\{\sum_{\alpha\gamma} z_{\alpha}^2z_{\gamma}^2F^{\alpha\gamma}(k,t)\right\}\times\left\{\frac{1}{k^2}\sum_{\alpha\gamma} z_{\alpha}z_{\gamma}F^{\alpha\gamma}(k,t)\right\}, \tag{6}$$

where we neglect the contribution of the second term of Eq. (3), since it behaves as $\mathcal{O}(k^2)$ in the low-wavelength region, whereas the first term is the order of unity. The first and the second factors represent the z^2-weighted number-density fluctuation and charge-density one, respectively. In particular, the initial value of $\zeta_{\text{Coulomb}}(t)$ is described as

$$\zeta_{\text{Coulomb}}(0)\propto\sum_{\mathbf{k}}\left\{\sum_{\alpha\gamma} z_{\alpha}^2z_{\gamma}^2\chi^{\alpha\gamma}(k)\right\}\times\left\{\frac{1}{k^2}\sum_{\alpha\gamma} z_{\alpha}z_{\gamma}\chi^{\alpha\gamma}(k)\right\}\sim\sum_{\mathbf{k}}\left\{\sum_{\alpha\gamma} z_{\alpha}^2z_{\gamma}^2\chi^{\alpha\gamma}(k)\right\}\left\{1-\frac{1}{\epsilon_L(k)}\right\}, \tag{7}$$

where $\chi^{\alpha\gamma}(k)=F^{\alpha\gamma}(k,t=0)$ is the static site–site structure factor, and $\epsilon_L(k)$ is the wave-number-dependent longitudinal dielectric constant.[21]

Based on Eq. (7), we can understand qualitatively how the interatomic strong Coulombic interaction leads to the pressure-induced enhancement of the molecular mobility. The second factor, $1-1/\epsilon_L(k)$, is almost independent of density, since it is already close to unity in the case of highly polar liquids and molten salts.[24] On the other hand, the first factor, which represents the z^2-weighted number-density fluctuation, is a decreasing function of density in the low-wave-number region, because the density fluctuation in the hydrodynamic limit is associated with the isothermal compressibility, and liquids usually become less compressible under higher pressure. Moreover, the right-hand side (rhs) of Eq. (7) should be divided by density in order to obtain the relaxation time of the charge density due to the density dependence of the inertia factor. As a result, the electrostatic friction on the charge-current density in the low-wave-number region decreases with increasing pressure, which leads to the increase in the dielectric relaxation rate or the electric conductivity if the effect of electrostatic friction is significant on the charge-current density. The decrease in the friction on the charge-current mode can enhance the relaxation of other dynamic modes through the dielectric friction or the relaxation of ionic atmosphere, to bring about the anomalous pressure dependence of various transport coefficients. In the previous study on water by Yamaguchi *et al.*, they analyzed their mode-coupling calculation and showed that the decrease in the electrostatic friction on the dielectric relaxation actually contribute to the anomalous pressure dependence of the dielectric relaxation time of water.[4]

The physical mechanism of the anomalous pressure dependence of the molecular mobility, explained mathematically above, is described schematically in the following way.

Consider the situation that the number-density fluctuation is induced in a liquid composed of highly polar molecules, as is shown in Fig. 1(a). When the polar molecules

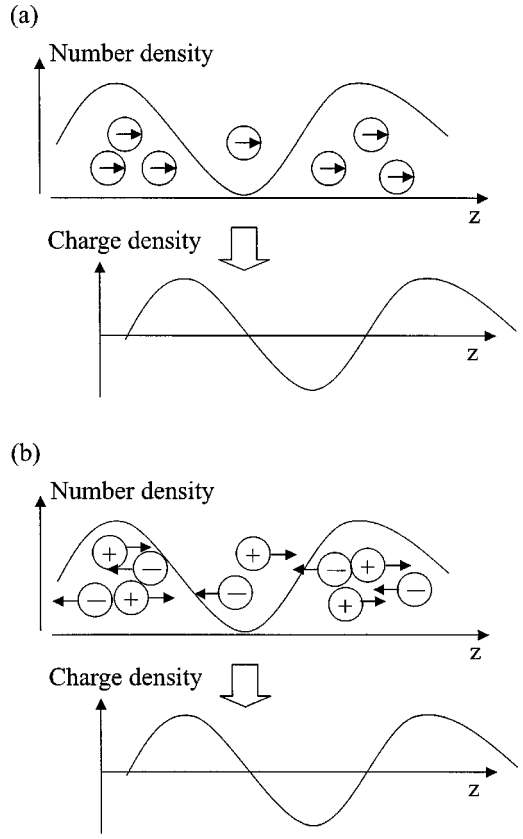

FIG. 1. Schematic picture on the electrostatic friction on the charge-current mode of (a) polar liquids and (b) molten salts. In (a), the uniform reorientation of the dipole moment leads to the heterogeneity of the charge density in the presence of the number-density fluctuation. In (b), the charge density fluctuation is caused by the relative displacement of cations and anions when the number density is not uniform.

are orientated in the z direction, there arises the gradient of the polarization density due to the number-density fluctuation. The heterogeneity of the polarization density stands for that of the charge density, whose electrostatic energy is proportional to $1-1/\epsilon$, which corresponds to the second factor of Eq. (7). Since the polarization along the z axis is unfavorable in the presence of the number-density fluctuation along the z axis by the mechanism above, the number-density fluctuation causes the friction on the dielectric mode through the Coulombic interaction.

A schematic picture can be drawn as Fig. 1(b) for molten salts. As is the case of polar liquids, the displacement of cations and anions in the opposite directions induces the charge-density fluctuation when the gradient of the number density is present. The charge density then leads to the increase in the Coulombic energy, so that the charge current is suppressed.

It should be noted here that, although the schematic pictures are different for polar molecular liquids and molten salts, we can treat both in the same formalism by employing the interaction-site description for molecular liquids.

B. Nernst–Einstein deviation parameter

The diffusion of ions in dilute electrolyte solutions is uncorrelated, and the ionic conductivity, σ, is given by the Nernst–Einstein relationship as follows:[21]

$$\sigma_{\mathrm{NE}}=\sum_{\alpha}\frac{\rho_{\alpha}z_{\alpha}^{2}D_{\alpha}}{k_{B}T}. \tag{8}$$

On the other hand, due to the correlation between the motions of ions, the Nernst–Einstein relationship does not hold in the case of concentrated electrolyte solutions and molten salts. In such a case, the Nernst–Einstein deviation parameter, denoted as Δ_{NE}, is defined in order to describe the deviation from the Nernst–Einstein relationship as[21]

$$\sigma=\sigma_{\mathrm{NE}}(1-\Delta_{\mathrm{NE}}). \tag{9}$$

The positive value of Δ_{NE} means that the collective ionic conduction is suppressed compared with the single-particle diffusion, and *vice versa*.

The deviation parameters of concentrated electrolyte solutions are often positive, which can be explained by the ion-pair formation. The value of Δ_{NE} is also positive in the case of many ionic liquids, and it has been attributed to the short-lived ion-pair formation.[21,25]

However, there are some cases where the Nernst–Einstein deviation parameters of ionic liquids become negative. For example, Trullàs *et al.* showed in their MD simulation that the deviation parameter of molten noble-metal halides are negative.[26,27] The deviation parameter of molten silica is also negative in the MD simulation at 4 g/cc and 4000 K.[28] Wilke *et al.* showed that the deviation parameter of the low-density ionic fluid becomes negative in their mode-coupling calculation, although they did not present the reason explicitly (the inset of Fig. 11 in Ref. 20). Very recently, we performed a MD simulation of molten LiBr, and showed that its Δ_{NE} is also negative, which is consistent with the experimental data. We further demonstrated that the negative deviation parameter can be reproduced by the mode-coupling calculation.[19] Since it is unlikely that the ions of the same charge can form the ion pair, it is necessary to construct another physical picture to elucidate the negative deviation parameter.

In this section we will show that the negative value of Δ_{NE} can be explained in a consistent way with the mechanism of the anomalous pressure dependence of transport properties described in the preceding section. Since the negative deviation parameter is observed in liquids whose transport properties depend on pressure in an anomalous way, we consider that a consistent elucidation of both the pressure dependence and the deviation parameter will support the validity of the mechanism.

Based on the fluctuation–dissipation idea, the frictional force on the charge-current density is described as Eq. (1). Due to the correlation between the random forces on different ions, the friction on the collective mode is not given by the sum of the individual ions as

$$\zeta^{s}(t)=\frac{1}{V}\left\langle \sum_{\alpha} z_{\alpha}^{2}\sum_{i\in\alpha}\mathbf{f}_{i}(t=0)\cdot\mathbf{f}_{i}(t)\right\rangle . \tag{10}$$

The collective ionic conduction is likely to be suppressed in comparison with the individual ionic motion ($\Delta_{\mathrm{NE}}>0$) when $\zeta(t)$ is larger than $\zeta^{s}(t)$, and *vice versa*.

In the similar way as the preceding section, the Coulombic part of $\zeta^{s}(t)$ is derived as

$$\zeta^s_{\mathrm{Coulomb}}(t) \propto \sum_{\mathbf{k}} \left\{ \sum_{\alpha} z_\alpha^4 F^{s,\alpha\alpha}(k,t) \right\} \times \left\{ \frac{1}{k^2} \sum_{\alpha\gamma} z_\alpha z_\gamma F^{\alpha\gamma}(k,t) \right\}, \tag{11}$$

where $F^{s,\alpha\gamma}(k,t)$ is the self-part of the partial dynamic structure factor defined as

$$F^{s,\alpha\gamma}(k,t) \equiv \frac{1}{N_\alpha} \sum_{i\in\alpha} \langle \exp[i\mathbf{k}\cdot(\mathbf{r}_i(t)-\mathbf{r}_i(0))] \rangle \delta_{\alpha,\gamma}. \tag{12}$$

Here N_α denotes the number of α atom.

Comparing Eq. (11) with Eq. (6), the collective dynamic structure factor in the first factor on the rhs of Eq. (6) is replaced by its self-part in Eq. (11). The self-part of the structure factor of dense liquids is usually larger than the collective part in the low-wave-number region where the Coulombic interaction is effective. Therefore, the electrostatic friction on the collective charge-current density becomes smaller than that expected from the sum of the uncorrelated motion of the individual ions, which is in favor of the negative value of the Nernst–Einstein deviation parameter.

Physically speaking, the electrostatic friction on the single-particle diffusion stands for the friction caused by the retarded relaxation of the ionic atmosphere. The displacement of a single ion is always accompanied by the change in the charge density, requiring the relaxation of the ionic atmosphere around the ion. On the other hand, the collective charge current does not lead to the change in the charge density of the liquid if the number density of the liquid is homogeneous, which leads to the relatively weak electrostatic friction on the collective charge-current mode.

III. THEORY

According to the general procedure of the projection operator formalism, one can derive the generalized Langevin equation for the dynamic structure factor of atomic liquid mixtures and its self-part, $\mathbf{F}(k,t)$ and $\mathbf{F}^s(k,t)$, respectively, as follows:[22,29,30]

$$\ddot{\mathbf{F}}(k,t) + k^2 \mathbf{J}\boldsymbol{\chi}^{-1}(k)\mathbf{F}(k,t) + \int_0^t d\tau\, \mathbf{K}(k,t-\tau)\mathbf{F}(k,\tau) = \mathbf{0}, \tag{13}$$

$$\ddot{\mathbf{F}}^s(k,t) + k^2 \mathbf{J}^s\mathbf{F}^s(k,t) + \int_0^t d\tau\, \mathbf{K}^s(k,t-\tau)\mathbf{F}^s(k,\tau) = \mathbf{0}. \tag{14}$$

The current correlation matrix and its self-part, $\mathbf{J}$ and $\mathbf{J}^s$, respectively, are given by

$$J^{\alpha\gamma} = \frac{\rho_\alpha k_B T}{m_\alpha}\delta_{\alpha\gamma}, \tag{15}$$

$$J^{s,\alpha\gamma} = \frac{k_B T}{m_\alpha}\delta_{\alpha\gamma}, \tag{16}$$

where m_α and ρ_α stand for the mass and the number density of the α atom, respectively.

The memory functions, denoted as $\mathbf{K}(k,t)$ and $\mathbf{K}^s(k,t)$ in Eqs. (13) and (14), respectively, are the generalized friction coefficients for $\mathbf{F}(k,t)$ and $\mathbf{F}^s(k,t)$. In the mode-coupling theory, the memory function is approximated as the linear combination of the quadratic form of the dynamic structure factor or its self-part as[22,29,30]

$$\rho_\alpha[\mathbf{J}^{-1}\cdot\mathbf{K}_{\mathrm{MCT}}(k,t)]_{\alpha\gamma}\rho_\gamma = \frac{1}{8\pi^3}\int d\mathbf{q}\{q_z^2[\mathbf{c}(q)\cdot\mathbf{F}(q,t)\cdot\mathbf{c}(q)]_{\alpha\gamma} \times \mathbf{F}^{\alpha\gamma}(|\mathbf{k}-\mathbf{q}|,t) - q_z(k-q_z)[\mathbf{c}(q) \cdot\mathbf{F}(q,t)]_{\alpha\gamma}[\mathbf{F}(|\mathbf{k}-\mathbf{q}|,t)\cdot\mathbf{c}(|\mathbf{k}-\mathbf{q}|)]_{\alpha\gamma}\}, \tag{17}$$

$$[\mathbf{J}^{s,-1}\mathbf{K}^s_{\mathrm{MCT}}(k,t)]_{\alpha\gamma} = \frac{1}{8\pi^3}\int d\mathbf{q}\, q_z^2[\mathbf{c}(q)\cdot\mathbf{F}(q,t)\cdot\mathbf{c}(q)]_{\alpha\gamma}\mathbf{F}^{s,\alpha\gamma}(|\mathbf{k}-\mathbf{q}|,t), \tag{18}$$

where $\mathbf{c}(q)$ is the direct correlation function, which stands for the effective intermolecular interaction between atoms, and z denotes the direction of $\mathbf{k}$.

In particular, the memory function for the hydrodynamic modes, $\mathbf{K}(k=0,t)$ and $\mathbf{K}^s(k=0,t)$, are given by

$$\rho_\alpha[\mathbf{J}^{-1}\cdot\mathbf{K}(k=0,t)]_{\alpha\gamma}\rho_\gamma = \int_0^\infty 4\pi q^2\, dq\, \kappa^{\alpha\gamma}(q,t), \tag{19}$$

$$[\mathbf{J}^{s,-1}\cdot\mathbf{K}^s(k=0,t)]_{\alpha\gamma} = \int_0^\infty 4\pi q^2\, dq\, \kappa^{s,\alpha\gamma}(q,t), \tag{20}$$

where $\boldsymbol{\kappa}(q,t)$ and $\boldsymbol{\kappa}^s(q,t)$ are the contribution to the time-dependent friction coefficient from the liquid structure of each wave number given by

$$\kappa^{\alpha\gamma}(q,t) = \frac{q^2}{24\pi^3}\{[\mathbf{c}(q)\cdot\mathbf{F}(q,t)\cdot\mathbf{c}(q)]_{\alpha\gamma}\mathbf{F}^{\alpha\gamma}(q,t) - [\mathbf{c}(q)\cdot\mathbf{F}(q,t)]_{\alpha\gamma}[\mathbf{F}(q,t)\cdot\mathbf{c}(q)]_{\alpha\gamma}\}, \tag{21}$$

$$\kappa^{s,\alpha\gamma}(q,t) = \frac{q^2}{24\pi^3}[\mathbf{c}(q)\cdot\mathbf{F}(q,t)\cdot\mathbf{c}(q)]_{\alpha\gamma}\mathbf{F}^{s,\alpha\gamma}(q,t). \tag{22}$$

In Eqs. (17) and (18), the values of $\mathbf{F}(k,t)$ and $\mathbf{F}^s(k,t)$ can be evaluated from $\mathbf{K}(k,\tau)$ and $\mathbf{K}^s(k,\tau)$ at $\tau<t$, which is determined by $\mathbf{F}(k,\tau)$ and $\mathbf{F}^s(k,\tau)$ in turn. In short, we can obtain the dynamic structure factor and its self-part at time t from those at $\tau<t$. Utilizing this property, we can calculate the dynamic structure factor in the whole time region from only the knowledge of the static structure factor, $\boldsymbol{\chi}(q)$, and that of the inertia, $\mathbf{J}$ and $\mathbf{J}^s$. If we use the integral equation theory for the equilibrium structure, as is done in this work, the static structure factor is obtained from the interionic interaction in turn. In such a case, we can evaluate the transport properties of ionic liquids from the input data of ionic masses, interionic interactions, temperature, and density only.

IV. MODEL AND NUMERICAL METHODS

In this work, we employ the modified Born–Mayer–Huggins potential with Tosi–Fumi parameter (hereafter called BMH potential) as the interionic interaction potential of molten alkali halides (LiBr and RbBr).[31] The BMH model has long been used in the MD simulation of alkali halides. The effective charges of ions in the BMH model are $\pm e$, where $-e$ is the charge of the electron, and the effect of electronic polarization is not included. Although the polarization of anion is thought to affect many properties of molten salts quantitatively, we consider that the rigid ion model is sufficient to understand the phenomena qualitatively. The interionic potential proposed by van Beest, Kramer, and van Santen (BKS potential) is employed for the silica melt, whose parameters are determined by *ab initio* quantum-chemical calculations.[32] The effective charges of Si and O ions are $+2.4e$ and $-1.2e$, respectively, and the polarization effect is not included. The short-range correction of Saika–Voivod *et al.* is employed in order to avoid the anomaly at the origin.[33] The BKS potential has been used for the MD simulations of molten silica and silica glass as one of the representative potential of silica.[14,33–40] In particular, it is reported by MD simulation studies that the BKS potential works well in reproducing the characteristic pressure dependence of the transport properties of silica melt.[14]

The equilibrium structure is calculated from the interionic potential using the Ornstein–Zernike (OZ)/hypernetted-chain (HNC) integral equation,[21] as is the case of the previous study on water by Yamaguchi *et al.*[4] The HNC equation is reported to work well in the case of molten alkali halides.[19,21,25]

The dynamic structure factor is calculated from the static structure using the generalized Langevin/mode-coupling theory described in the preceding section. Although the mode-coupling approximation is the approximation for the long-time part of the memory function,[21–23] we used the mode-coupling expression in the whole-time region. We consider that this approximation will not affect the qualitative mechanism of the transport properties, since their anomalous pressure dependence is reproduced well as will be exhibited later. In the numerical procedure, the reciprocal space is linearly discretized as $k=(n+\frac{1}{2})\Delta k$, where n is the integer from 0 to N_k-1. The number of grids, N_k, is 128 for LiBr and SiO_2, and 256 for RbBr. The spacings in the reciprocal space, Δk, are 0.245, 0.163, and 0.061 $Å^{-1}$ for LiBr, SiO_2, and RbBr, respectively.

The time development of the correlation function in the hydrodynamic limit, $k\to 0$, is separately treated by the analytical limiting procedure of the theoretical expressions in order to obtain the transport coefficients. The relationship between the dynamic structure factor and the transport coefficients is described elsewhere.[4,21]

V. RESULTS AND DISCUSSIONS

A. LiBr: The simplest case

We will demonstrate our numerical results on molten LiBr in this section. Parts of the results are already shown in our previous letter.[19] All the calculations shown here are performed at 1000 K. Although results at other temperatures were exhibited in the previous letter,[19] they are omitted here, since temperature dependence is not within the scope of our present work.

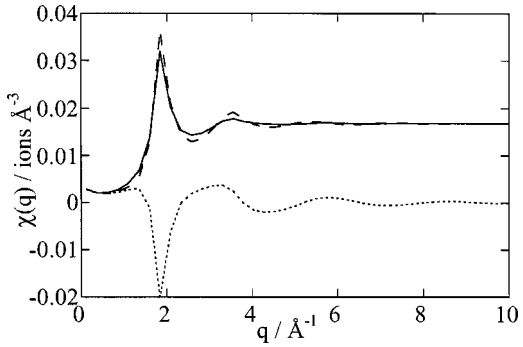

FIG. 2. Static structure factor of molten LiBr at 0.01677 ions/$Å^3$ and 1000 K. The solid, dotted, and dashed lines denote $\chi_{++}(q)$, $\chi_{+-}(q)$, and $\chi_{--}(q)$, respectively.

Figure 2 shows the partial structure factors, $\boldsymbol{\chi}(q)$, at 1 atm (the number density of each ion is 0.016 77 ions/$Å^3$).[41] The density dependence of the local counter-ion density, which is defined as the radial distribution function multiplied by the number density, is exhibited in Fig. 3. As is shown in Fig. 3, the coordination number of the counter ion is an increasing function of density. Therefore, the collision frequency increases with increasing density, so that the ionic mobility is expected to decrease with density based on the Enskog idea.

The molar ionic conductivity and the diffusion coefficients, obtained by the mode-coupling calculation, are shown in Fig. 4. The relative change from the values at the ambient pressure is plotted. Contrary to the expectation from the coordination number, the molar ionic conductivity is an increasing function of the density in the low pressure region, which is consistent with the experimental observations.[16,17] The absolute values of the molar conductivity and diffusion coefficients at 1 atm are shown in Table I. The theory underestimates the conductivity by about 30% compared with the experiment.[17] We consider this agreement is satisfactory because only the interionic interaction potential is used as input data in our theory.

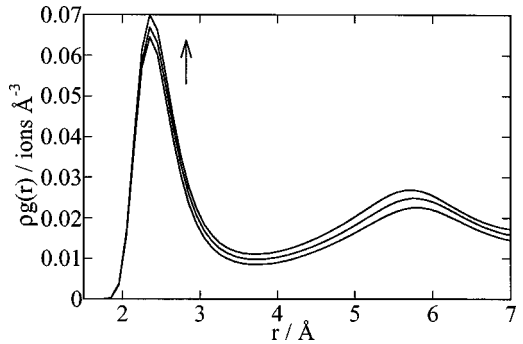

FIG. 3. Local counter-ion density of molten LiBr, defined as $\rho g_{+-}(r)$, at 0.016 77, 0.018 45 and 0.020 12 ions/$Å^3$. The arrow indicates the direction of increasing density.

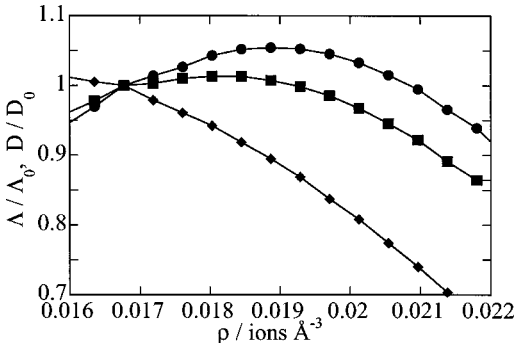

FIG. 4. The relative change in the diffusion coefficients (D) and molar conductivity (Λ) of molten LiBr with respect to those at 1 atm (0.016 77 ions/Å^3), denoted as D_0 and Λ_0, respectively. The circles stand for the molar conductivity, and the squares and diamonds indicate the diffusion coefficients of cation and anion, respectively.

Comparing the density dependence of the molar conductivity with those of single-particle diffusion coefficients of ions in Fig. 4, the increase in the mobility is stronger for the collective ionic conduction than for the single-particle diffusion. It clearly indicates that the anomaly in the density dependence of the transport coefficients of molten LiBr stems from the collective charge-density mode, rather than the single-ionic motions, and it is also consistent with the physical picture presented in Sec. II. The decrease in the diffusion coefficient with density is weaker for cation, because the effect of ionic atmosphere is larger for smaller Li^+ ion. The relative density dependence of the diffusion coefficients of cation and anion is consistent with the MD simulation reported by Okada *et al.*[18]

In the MD simulation of Okada *et al.*, the diffusion coefficient of Li^+ is a weakly decreasing function of density,[18] whereas it shows slight increase in our theoretical calculation. The diffusion coefficient of Li^+ ion in molten LiBr has yet to be measured to our best knowledge, and we consider it is worthy of experiment, although the precise measurement of the diffusion coefficient under the high-temperature, high-pressure condition is difficult. As for the discrepancy between the simulation and the theory with respect to the pressure dependence of the cationic diffusion coefficient, we consider it is not an essential failure of our theory. First, the increase in the diffusion coefficient is so small in our theory that it may be buried under the statistical error of the simulation. Second, since our theory exaggerates the increase in the molar conductivity compared with experiments, the increase in the cationic diffusion coefficient is also likely to be overestimated, and the maximum of the diffusion coefficient may appear only in the negative pressure region where the simulation was not performed.

TABLE I. The ionic diffusion coefficients, the molar conductivities (Λ), and the Nernst–Einstein deviation parameters of molten LiBr (1000 K) and RbBr (1075 K) at 1 atm from the theoretical calculation.

	$D_+/10^{-5}$ cm^2 s^{-1}	$D_-/10^{-5}$ cm^2 s^{-1}	Λ/cm^2 mol^{-1} Ω^{-1}	Δ
LiBr	6.8	3.7	134	−0.13
RbBr	1.7	1.7	31.2	+0.17

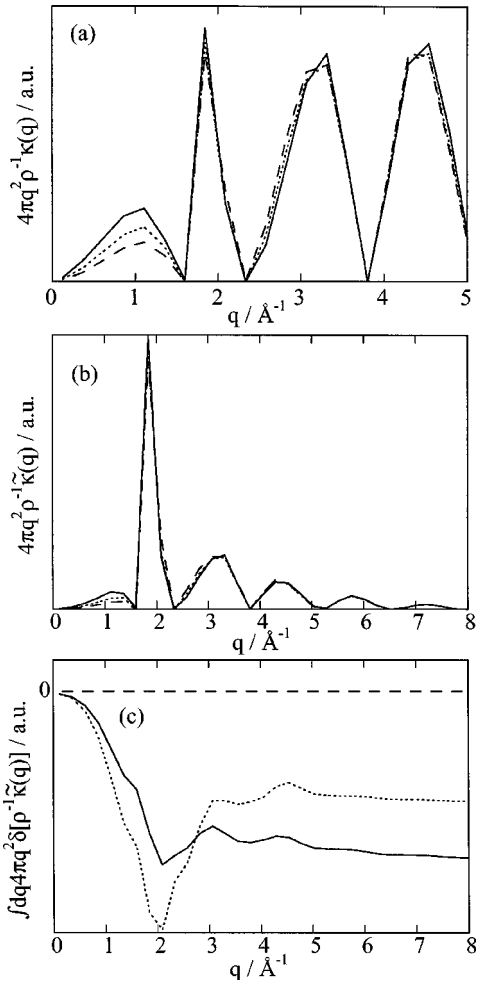

FIG. 5. Dielectric part of (a) $4\pi q^2\rho^{-1}\kappa(q)$ and (b) $4\pi q^2\rho^{-1}\tilde{\kappa}(q)$ of molten LiBr. See the text for the definition of the functions. Solid, dotted, and dashed curves denote the functions at 0.016 77, 0.018 45, and 0.020 12 ions/Å^3, respectively. In (c), the running integrals of the difference of $4\pi q^2\rho^{-1}\tilde{\kappa}(q)$ from that at 0.016 77 ions/Å^3 are plotted. The solid and dotted curves refer to those at 0.018 45 and 0.020 12 ions/Å^3, respectively.

As was discussed in the previous work on water by Yamaguchi *et al.*, the initial value of $\boldsymbol{\kappa}(q,t)$, defined by Eq. (21), can be regarded as the distortion of the liquid structure accompanying the ionic conduction.[4] We show the density dependence of $\boldsymbol{\kappa}(q)\equiv\boldsymbol{\kappa}(q,t=0)$ in Fig. 5(a). Only the dielectric component is plotted there, since all the components are proportional to the dielectric one in the case of binary ionic mixture due to the momentum conservation. Since $\mathbf{J}$ is proportional to ρ, the factor of ρ^{-1} is multiplied so that observed density dependence corresponds to that of the relaxation time, where ρ stands for the molar density. The mode-density factor, $4\pi q^2$, is also multiplied there.

In Fig. 5(a), the structure below 1.5 Å^{-1} mainly comes from the Coulombic interaction as is elucidated in Sec. II, whereas the higher wave-number part can be attributed to the short-range repulsive interaction. Although not shown explicitly, the density dependence of the static structure below 1.5 Å^{-1}, in particular at $0<q<1$ Å^{-1}, has the same characteristics with that at $q=0$ in that the number-density fluctuation is supressed by the packing effect while the charge density one is almost invariant. As is expected, the friction from

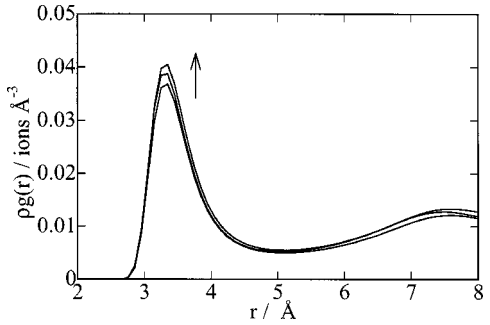

FIG. 6. Local counter-ion density of molten RbBr at 0.009 38, 0.009 92, and 0.010 32 ions/Å^3. The arrow indicates the direction of increasing density.

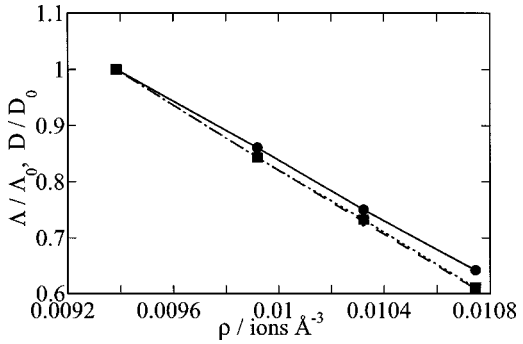

FIG. 7. Relative change in the molar conductivity and the diffusion coefficients of molten RbBr with respect to those at 1 atm (0.009 38 ions/Å^3). All marks are the same as those of Fig. 4. The squares and diamonds are almost overlapped with each other in the figure.

the low-wave-number region decreases with increasing density due to the decrease in the number-density fluctuation. On the other hand, the high-wave-number part is almost invariant and slightly increases with density. We consider it is due to the relatively small increase in the coordination number of the counter ions with density, as is shown in Fig. 3.

Figure 5(b) demonstrates the time-integrated wave-number-resolved memory function as

$$\tilde{\boldsymbol{\kappa}}(q) \equiv \int_0^\infty dt\, \boldsymbol{\kappa}(q,t), \tag{23}$$

multiplied by the same factor as Fig. 5(a). By integrating over q, it directly generates the zero-frequency friction on the zero-wave-number ionic charge current. The running integral of the difference of $\tilde{\boldsymbol{\kappa}}(q)$ from that of the ambient pressure is plotted in Fig. 5(c), in order to demonstrate the origin of the decrease in friction clearly.

As is seen in Figs. 5(b) and 5(c), the density dependence of $\tilde{\boldsymbol{\kappa}}(q)$ inherits that of the initial time in a rather straightforward way. Although the absolute contribution of the high-wave-number region is large, its density dependence is quite small, and more than half of the decrease in the zero-frequency friction comes from that of the low-wave-number region ($q<1.5\,\text{Å}^{-1}$). The decrease in the contribution of the high-q region in Fig. 5(c) may be attributed partly to the coupling with the charge-density modes. At the density higher than 0.019 ions/Å^3, the contribution of the repulsive interaction begins to increase, which leads to the decrease in the molar conductivity.

B. RbBr: The distinction between normal and anomalous pressure dependence

In this section, we will present the density dependence of the transport coefficients of molten RbBr obtained in the same way as those of LiBr. Since the ionic mobilities of molten RbBr is reported experimentally to be a decreasing function of pressure,[16] the comparison between LiBr and RbBr will help answer the question what is the characteristics of LiBr among other molten salts that leads to the anomaly in the pressure dependence of the transport properties.

All the calculations on molten RbBr are performed at 1075 K and various densities from 0.009 384 ions/Å^3 (the number density of each ion at 1 atm[41]) to 0.010 746 ions/Å^3.

Figure 6 shows the local counter-ion density at three different densities. The coordination number of the counter ion is an increasing function of density. Compared with that of molten LiBr (Fig. 3), the increase in the coordination number is larger in the case of RbBr, given that the overall increase in the bulk density is 20% and 10% in Figs. 3 and 6, respectively.

The density dependence of the molar conductivity and diffusion coefficients is plotted in Fig. 7. They are normalized to the values at the ambient pressure, which are summarized in Table I. Contrary to the molten LiBr (Fig. 4), all the transport coefficients are decreasing functions of density, consistent with the experiment.[16] The agreement of the absolute value of the transport coefficients with the experiment is worse than that of LiBr, which we consider may partly be attributed to the performance of the BMH potential in the case of RbBr. All the transport coefficients behave similarly by compression, and it looks as if all of them are controlled by the same parameter such as viscosity, although the coupling with the transverse current density is not included in our calculation.

The density dependence of $\boldsymbol{\kappa}(q)$ is exhibited in Fig. 8. Owing to the general mechanism described in Sec. II, the contribution from the low-wave-number region (<1 Å^{-1}) decreases with increasing density. Compared with the corresponding functions of LiBr [Fig. 5(a)], however, $\boldsymbol{\kappa}(q)$ of

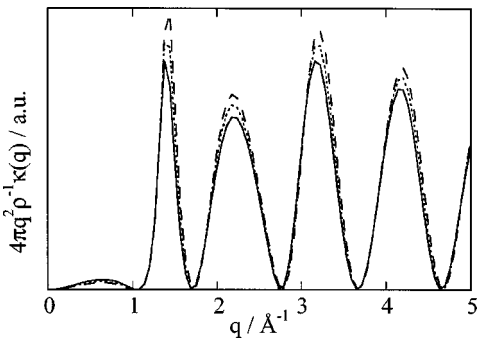

FIG. 8. Dielectric part of $4\pi q^2 \rho^{-1} \boldsymbol{\kappa}(q)$ of molten RbBr. Solid, dotted, and dashed curves denote the functions at 0.009 38, 0.009 92 and 0.010 32 ions/Å^3, respectively.

RbBr is different in the following two features, so that the ionic mobility decreases with increasing density.

First, the relative contribution of the low-wave-number region to the whole friction is quite small in the case of RbBr. It indicates that the Coulombic interaction plays only a minor role in the frictional force on the ionic conduction, which can be explained in terms of the difference in the size of cation.

Second, $\boldsymbol{\kappa}(q)$ in the high-q region is strongly dependent on density. Since the high-q part corresponds to the short-range repulsive interaction, its large increase corresponds to the rapid increase in the counter-ion coordination number as is shown in Fig. 6. The difference in the density dependence of the local structure, in turn, may stem from the difference in the interatomic interaction to determine the structure qualitatively, that is, the importance of the attractive Coulombic interaction is larger on LiBr than on RbBr.

In summary, the two ionic liquids investigated here, LiBr and RbBr, share the same mechanism that the electrostatic friction on the collective ionic current can decrease with increasing pressure through the decrease in the number-density fluctuation in the low-wave-number region. At the same time, both liquids also have another mechanism in common, that the repulsive friction increases with increasing pressure due to the increase in the coordination number. The difference between LiBr and RbBr appears quantitative rather than qualitative in our calculation. In the case of LiBr, the former mechanism is relatively strong and the latter one is very weak, so that the former one appears in the resultant transport coefficient, whereas the former is usually dominated by the latter in most ionic liquids. A detailed knowledge of the liquid structure will be required to understand in what condition the density dependence of the electrostatic friction may lead to the pressure-induced enhancement of the molecular mobility without the disturbance of the repulsive interaction.

C. Nernst–Einstein deviation parameter

The Nernst–Einstein deviation parameters, Δ_{NE}, of LiBr and RbBr obtained by the theory are shown in Table I. As is the case of other alkali halides,[25] Δ_{NE} is positive for RbBr, which indicates that the collective ionic conduction is *suppressed* compared with the single-ionic diffusion. On the other hand, Δ_{NE} of molten LiBr is negative in our theory, and it is consistent with a simulation and experiments.[19] In Sec. II we have presented a physical mechanism on the negative deviation parameter, which is in harmony with the anomalous pressure dependence of ionic conductivity. In this section, we show the analysis of our theoretical calculation based on the mechanism in Sec. II.

Figure 9 shows the time-integrated wave-number-resolved friction coefficient and its self-part, defined as

$$4\pi q^2\rho^{-1}\tilde{\kappa}(q)\equiv\frac{q^4}{6\pi^3\rho}\int_0^\infty dt\sum_{\alpha\gamma} z_\alpha z_\gamma\{[c(q)\cdot\mathbf{F}(q,t)\cdot\mathbf{c}(q)]_{\alpha\gamma}\mathbf{F}^{\alpha\gamma}(q,t)-[\mathbf{c}(q)\cdot\mathbf{F}(q,t)]_{\alpha\gamma}[\mathbf{F}(q,t)\cdot\mathbf{c}(q)]_{\alpha\gamma}\} \tag{24}$$

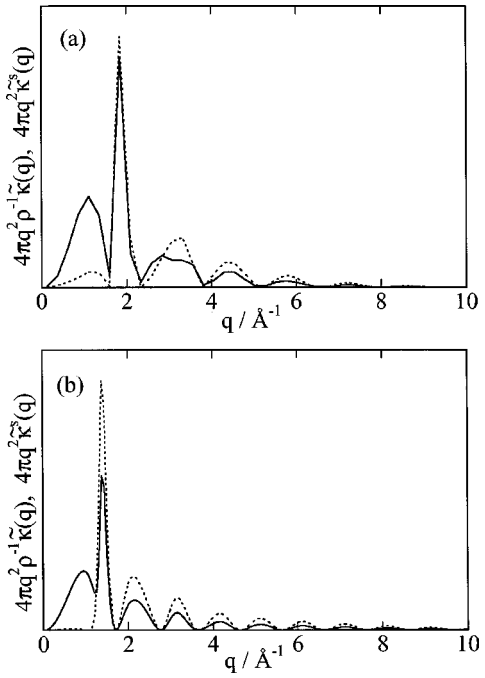

FIG. 9. Comparison between the dielectric part of $4\pi q^2\rho^{-1}\tilde{\kappa}(q)$ [Eq. (24)] and its self-part, Eq. (25). The former and the latter are drawn as the dotted and solid curves, respectively. The functions for LiBr and RbBr are shown in (a) and (b), respectively.

and

$$4\pi q^2\tilde{\kappa}^s(q)\equiv\frac{q^4}{6\pi^3\rho}\int_0^\infty dt\sum_{\alpha\gamma} z_\alpha z_\gamma[\mathbf{c}(q)\cdot\mathbf{F}(q,t)\cdot\mathbf{c}(q)]_{\alpha\gamma}\mathbf{F}^{s,\alpha\gamma}(q,t), \tag{25}$$

respectively, where $\rho\equiv\rho_+=\rho_-$. According to the discussion in Sec. II B, the difference between them represents the distinct part of the memory function resolved into the contribution of each wave number.

As is expected from the discussion in Sec. II B, the self-part exceeds the collective one in the low-q region. On the other hand, the former is smaller than the latter in the high-q region, which can be attributed to the fact that the short-range repulsive interaction is likely to act between a cation and an anion. The contribution of the former is relatively large and the difference between two functions is small in the high-q region in the case of LiBr, which leads to the negative value of the Nernst–Einstein deviation parameter.

Trullàs and Padró proposed in their MD simulation work on molten noble-metal halides that the negative value of the deviation parameter originates in the collision between larger anions.[26] Their explanation appears different from ours at first glance, since the negative deviation parameter always comes from the low-q region, not from the high-q one that represents the collisional interaction. In addition to the relative contribution of the electrostatic and repulsive interactions, however, the difference between the collective and the self-functions in the high-q region is smaller for LiBr in comparison with RbBr, and we consider it may have something to do with the repulsive interaction between larger anions.

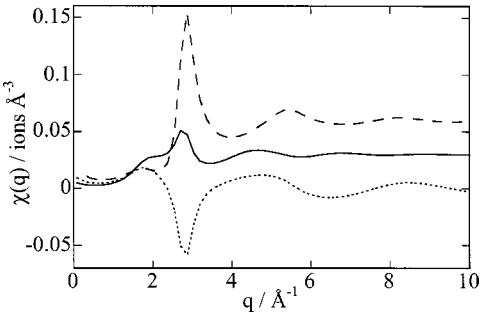

FIG. 10. The static structure factor of molten silica at 0.0300 ions/Å^3 (number density of Si atom) and 3000 K. All the symbols are the same as in Fig. 2.

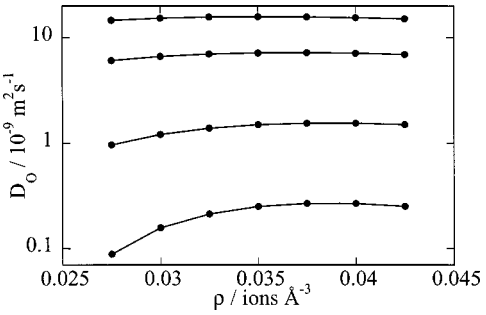

FIG. 11. The theoretical self-diffusion coefficient of oxygen in silica melt is plotted against density. The temperature of the system is, from lower to upper, 3000, 4000, 6000, and 8000 K, respectively.

D. Silica: The revival of the conventional picture

This section deals with the ionic mobility of molten silica. The temperature and the density of the systems calculated are 3000–8000 K and 0.0275–0.0425 ions/Å^3 (the number density refers to that of the Si atom here), respectively. Although the density of silica melt is less than 0.025 ions/Å^3 at the ambient pressure,[42] we cannot perform the calculation in the lower-density region, because the OZ/HNC integral equation is not convergent numerically there. In the mode-coupling calculation of Sciortino and Kob, they reported that the ideal glass-transition temperature of silica melt is largely affected by the inclusion of the three-body direct correlation function.[38] Due to the lack of the information on the three-body correlation in the integral equation theory, however, we employed the ordinary expression of the memory function, not including the three-body direct correlation function. We believe we can extract the physical mechanism of the anomalous pressure dependence of the ionic mobility of silica melt from our theoretical calculation without the three-body direct correlation function, so long as it can reproduce the characteristic pressure dependence of the mobility qualitatively.

Figure 10 shows the partial static structure factor at 3000 K and 0.0300 ions/Å^3. Compared with the structure factor of molten LiBr (Fig. 2), it should be noticed that the small peak (shoulder) is found around 2 Å^{-1}. This peak is more evident in experiments and simulations of silica and related materials in lower-temperature, lower-density region, and it is called ''prepeak'' or ''first sharp diffraction peak'' (FSDP).[43–47] In contrast to the peak around 3 Å^{-1}, the density fluctuation modes of Si and O ions are positively correlated in FSDP, which indicates that FSDP is associated with the fluctuation of the charge-neutral cluster of ions, i.e., SiO_2 unit.

Figure 11 demonstrates the diffusion coefficient of O atom obtained by our theory. Compared with the corresponding MD simulation performed by Shell *et al.* using the same potential,[14] the characteristic behavior of the diffusion coefficient is reproduced qualitatively well, although the absolute value of the diffusion coefficient is several times smaller. The diffusion coefficient of Si atom and the shear viscosity also show the similar anomalous pressure dependence in our theory, although they are not plotted here.

Figure 12(a) exhibits the z^2-weighted number-density fluctuation and the charge-density fluctuation at 3000 K and two different densities, 0.0300 and 0.0350 ions/Å^3, where the weighting factor of z^2 corresponds to Eq. (7). The factor of ρ^{-1} is multiplied to the z^2-weighted number-density fluctuation for normalization. Owing to the positive correlation between the Si and O modes, FSDP structure appears strongly in the number-density fluctuation. On the other hand, the charge-density mode is suppressed up to FSDP, which means that the charge neutrality is maintained at the FSDP mode, and at the same time the interionic Coulombic potential is effective up to 2 Å^{-1}. The FSDP decreases with increasing density in the low-wave-number region and apparently shifts to higher wave number, which is consistent with the x-ray diffraction of silica glass.[44]

Figure 12(b) plots the functions that correspond to Fig. 5(a) for molten LiBr. Both functions resemble each other qualitatively in that the contribution of the low-wave-number structure is a decreasing function of density, whereas that of the peak of the structure factor (2 and 3 Å^{-1} for LiBr and

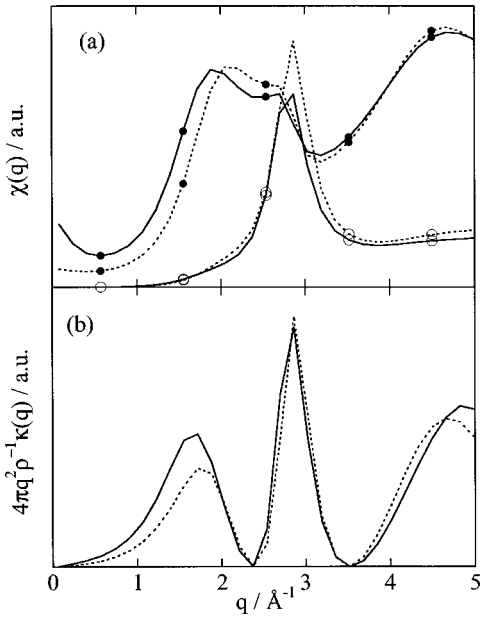

FIG. 12. (a) The z^2-weighted number-density fluctuation (solid circle) and the charge-density fluctuation (open circle) of silica at 3000 K. Solid and dotted curves denote those of 0.0300 and 0.0350 ions/Å^3, respectively. The number-density fluctuation is divided by the molar density for normalization. (b) Dielectric part of $4\pi q^2 \rho^{-1} \kappa(q)$ at 0.0300 (solid) and 0.0350 ions/Å^3.

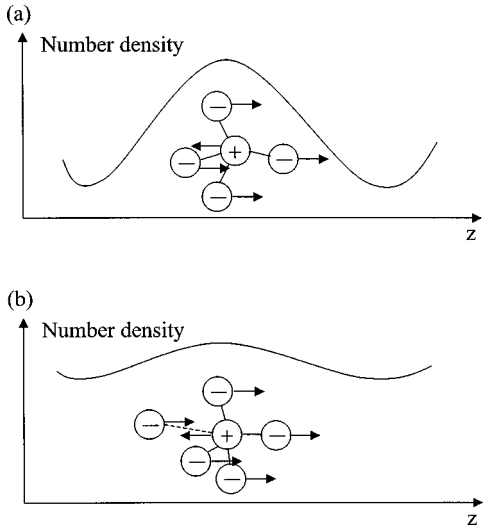

FIG. 13. A schematic picture of the anomalous pressure dependence of molten silica when special attention is paid to the role of the first sharp diffraction peak (FSDP). In the low-density region, there are definite tetrahedral SiO_2 units as is described in (a), which bring about FSDP. In such a case, the relative motion of Si and O atoms is restricted due to the large polarization energy of the SiO_2 unit. In the high-density region, however, the FSDP becomes smaller, and there can be another fifth O atom around the Si atom, as is described in (b). The electrostatic interaction between the fifth O atom and Si atom, denoted as the dotted line, can reduce the polarization energy mentioned above.

silica, respectively) is almost invariant. However, the major difference is that the peak of the low-wave-number structure exists on the low-wave-number side of the FSDP in the case of silica.

The electrostatic friction on the charge-current mode is the linear combination of the number- and charge-density modes according to Eq. (7). If the number-density fluctuation increases as FSDP in the low-wave-number region where the interionic Coulombic interaction is effective, it results in the increase in the frictional force on the charge-current mode. A similar behavior has been found in the previous study on water performed by Yamaguchi *et al.*, although it appears less clear partly because the RISM/HNC theory does not reproduce the characteristic double-peak structure in the static structure factor of water.[4] We consider that the absence of the contribution of the FSDP-like structure in the case of LiBr is one of the reason for the relatively small anomaly in the pressure dependence of its transport coefficients.

Based on the correlation between the coordination number and the ionic mobility, Angell *et al.* proposed that the Si atom coordinated by five O atoms is responsible for the increase of the ionic mobility.[11] We can draw the following corresponding picture if a special attention is paid to the role of the FSDP, although the definite distinction of the contribution of FSDP is difficult since the peak around 2 $Å^{-1}$ is broad and its edge continues to the low-wave-number limit.

Figure 13 shows the schematic picture that stresses on the number-density fluctuation around 2 $Å^{-1}$. As is described above, FSDP can be interpreted as the density fluctuation of SiO_2 units. Therefore, the presence of FSDP can be described schematically as Fig. 13(a). When the cation and the anion are pulled in the opposite direction, the SiO_2 unit has a large electric dipole moment, which requires large polarization energy. The electric current is hence not favored by the electrostatic energy. On the other hand, consider the situation that the number-density fluctuation is suppressed by the compression as is shown in Fig. 12(a), and the fifth O atom is located near the Si atom (connected by a broken line) as is described in Fig. 13(b). In such a case, the polarization energy of the SiO_2 unit is cancelled by the electrostatic energy between Si atom and the fifth O atom, and the electric current is electrostatically more favored compared with Fig. 13(a). We therefore consider that the physical picture of the anomalous pressure dependence of silica melt obtained by our theory is essentially consistent with that of Angell *et al.*[11] that the increase in the number of five-coordinated Si atoms is responsible for the increase in the ionic mobility. However, it should be mentioned here that the structural information we used is that on the uniaxial correlation functions, not including the angular distribution such as the bond-angle order explicitly.

Guissani and Guillot reported in their MD study on silica melt that the Nernst–Einstein deviation parameter is strongly negative ($\Delta_{NE} \sim -2$) at 4000 K and 4 g/cc (0.04 ions/$Å^3$), whereas it is positive in the low-temperature low-density region.[28] The negative value of the deviation parameter is consistent with the mechanism described in Sec. II B, and we actually obtained the negative deviation parameter ($\Delta_{NE} \sim -0.14$) at the corresponding state point. Although the absolute value is quite different, it may be attributed to various reasons such as the difference in the interaction potential, the insufficient structural information from the integral equation theory and so on. Though the calculation is not performed here in the low-temperature, low-density region, we consider that the positive deviation parameter does not contradict with the present mechanism, because the pronounced FSDP there will violate the condition that the collective number-density fluctuation is smaller than the single-particle one.

VI. CONCLUDING REMARKS

In this work, we have presented our mode-coupling calculation on the density dependence of the transport properties of three ionic liquids, LiBr, RbBr and silica. Two of them, LiBr and silica, show the increase in the ionic mobilities with increasing density in the low-pressure region, as is observed by the experiments or the simulations. The calculation is analyzed in the same way as the mode-coupling study of the anomalous pressure dependence of the molecular motion of water performed by Yamaguchi *et al.*,[4] in order to clarify the similarities of the physical mechanisms of the ionic liquids and water.

The pressure dependence of the ionic mobility of three ionic liquids is reproduced fairly well by the theoretical calculation. The Coulombic part of the friction on the collective electric current decreases with density due to the decrease in the number-density fluctuation, as is expected from the mechanism proposed for water. On the other hand, the density dependence of the contribution of the short-range (high-wave-number) structure is quite small in the case of LiBr and silica. As a result, the ionic mobility reflects the decrease in

the electrostatic friction in a straightforward manner, leading to its anomalous pressure dependence observed by experiments or simulations.

The electrostatic friction on the ionic conductivity of RbBr also decreases with increasing density, as is the case of LiBr. However, its absolute magnitude is so small that it hardly contributes to the total friction. Moreover, the contribution of the short-range part is a strongly increasing function of density due to the rapid increase in the coordination number, which dominates the increase in the total friction.

Although a picture similar to LiBr is obtained on silica melt, the large difference is that the electrostatic friction is enhanced by the presence of the FSDP in the low-wave-number region. If we focus on the role of the FSDP in particular, we can draw a scheme of the anomalous pressure dependence of transport properties consistent with the conventional picture that the Si atom coordinated by five O atoms enhances the ionic mobility.

In addition to the anomalous pressure dependence of the transport properties, we can also reproduce the negative value of the Nernst–Einstein deviation parameter reported by the MD simulation of LiBr[19] and silica.[28] The homogeneous ionic-charge current does not induce the charge heterogeneity in the absence of the number-density fluctuation. In contrast, the motion of a single ion is always accompanied by the change in the charge distribution, which requires the relaxation of the ionic atmosphere around the ion. Therefore, the Coulombic part of the frictional force is likely to be stronger on the single-ionic motion than on the collective charge current, which leads to the ionic conduction faster than the Nernst–Einstein relationship. On the other hand, the effect of the short-range interaction is stronger on the collective charge current, since the repulsive interaction is likely to act between a cation and an anion. The sign of the Nernst–Einstein deviation parameter is determined by the balance between the above two effects, and it can be negative when the Coulombic contribution to the frictional force is strong.

In summary, we have presented a possibility that various characteristic properties of some ionic liquids, such as the pressure-induced enhancement of the ionic mobilities or the ionic conduction faster than the Nernst–Einstein relationship, can be understood in terms of the general properties of the Coulombic part of the frictional force in dense liquids, as is the case of water proposed by Yamaguchi *et al.*[4] We hope that the present mechanism will also shed light on other curious properties of ionic liquids such as Chemla effect.[48,49]

ACKNOWLEDGMENTS

The authors are very grateful to Professor F. Hirata (Institute for Molecular Science) and Dr. S.-H. Chong (Université Montpellier II) for reading and commenting on the paper.

[1] D. Eisenberg and W. J. Kauzmann, *The Structure and Properties of Water* (Clarendon, London, 1969) and references therein.
[2] K. Tördheide, in *Water: A Comprehensive Treatise*, edited by F. Franks (Plenum, New York, 1972), Vol. 1, Chap. 13 and references therein.
[3] C. A. Angell, in *Water: A Comprehensive Treatise*, edited by F. Franks (Plenum, New York, 1982), Vol. 7, Chap. 1 and references therein.
[4] T. Yamaguchi, S.-H. Chong, and F. Hirata, J. Chem. Phys. **119**, 1021 (2003).
[5] I. Kushiro, J. Geophys. Res. **81**, 6347 (1976).
[6] I. Kushiro, H. S. Yoder, Jr., and B. O. Mysen, J. Geophys. Res. **81**, 6351 (1976).
[7] I. Kushiro, Earth Planet. Sci. Lett. **41**, 87 (1978).
[8] S. K. Sharma, D. Virgo, and I. Kushiro, J. Non-Cryst. Solids **33**, 235 (1979).
[9] B. O. Mysen, D. Virgo, and C. M. Scarfe, Am. Mineral. **65**, 690 (1980).
[10] N. Shimizu and I. Kushiro, Geochim. Cosmochim. Acta **48**, 1295 (1984).
[11] C. A. Angell, P. A. Cheeseman, and S. Tamaddon, Science **218**, 885 (1982).
[12] C. A. Angell, P. Cheeseman, and S. Tamaddon, Bull. Mineral. **106**, 87 (1983).
[13] C. A. Angell, P. A. Cheeseman, and R. R. Kadiyala, Chem. Geol. **62**, 83 (1987).
[14] M. S. Shell, P. G. Debenedetti, and A. Z. Panagiotopoulos, Phys. Rev. E **66**, 011202 (2002).
[15] L. V. Woodcock, C. A. Angell, and P. Cheeseman, J. Chem. Phys. **65**, 1565 (1976).
[16] B. Cleaver, S. I. Smedley, and P. N. Spencer, J. Chem. Soc., Faraday Trans. 1 **68**, 1720 (1972).
[17] K. Tödheide, Angew. Chem., Int. Ed. Engl. **19**, 606 (1980).
[18] I. Okada, A. Endoh, and S. Baluja, Z. Naturforsch., A: Phys. Sci. **46**, 148 (1991).
[19] T. Yamaguchi, A. Nagao, T. Matsuoka, and S. Koda, Chem. Phys. Lett. **374**, 556 (2003).
[20] S. D. Wilke, H. C. Chen, and J. Bosse, Phys. Rev. E **60**, 3136 (1999).
[21] J.-P. Hansen and I. R. McDonald, *Theory of Simple Liquids*, 2nd. ed. (Academic, London, 1990).
[22] U. Balucani and M. Zoppi, *Dynamics of the Liquid State* (Clarendon, Oxford, 1994).
[23] J. P. Boon and S. Yip, *Molecular Hydrodynamics* (McGraw–Hill, New York, 1980).
[24] We shall comment on that the wave-number-dependent dielectric constant, $\epsilon(q)$, enters in Eq. (7) as $1-\epsilon_L^{-1}(q)$. Although the value of $\epsilon_L(q)$ may be negative and change with density, the variation of $1-\epsilon_L^{-1}(q)$ is small so long as the absolute value of $\epsilon_L(q)$ is sufficiently larger than unity.
[25] J. P. Hansen and I. R. McDonald, Phys. Rev. A **11**, 2111 (1975).
[26] J. Trullàs and J. A. Padró, Phys. Rev. B **55**, 12210 (1997).
[27] J. Trullàs, O. Alcaraz, L. E. González, and M. Silbert, J. Phys. Chem. B **107**, 282 (2003).
[28] Y. Guissani and B. Guillot, J. Chem. Phys. **104**, 7633 (1996).
[29] J. Bosse and M. Henel, Ber. Bunsenges. Phys. Chem. **95**, 1007 (1991).
[30] J. Bosse and Y. Kaneko, Phys. Rev. Lett. **74**, 4023 (1995).
[31] M. J. L. Sangster and M. Dixon, Adv. Phys. **25**, 247 (1976).
[32] B. W. H. van Beest, G. J. Kramer, and R. A. van Santen, Phys. Rev. Lett. **64**, 1955 (1990).
[33] I. Saika-Voivod, F. Sciortino, and P. H. Poole, Phys. Rev. E **63**, 011202 (2001).
[34] I. Saika-Voivod, P. H. Poole, and F. Sciortino, Nature (London) **412**, 514 (2001).
[35] K. Vollmayr, W. Kob, and K. Binder, Phys. Rev. B **54**, 15808 (1996).
[36] R. G. Della Valle and E. Venuti, Chem. Phys. **179**, 411 (1994).
[37] S. D. Bembenek and B. B. Laird, J. Chem. Phys. **114**, 2340 (2001).
[38] F. Sciortino and W. Kob, Phys. Rev. Lett. **86**, 648 (2001).
[39] R. G. Della Valle and E. Venuti, Phys. Rev. B **54**, 3809 (1996).
[40] P. Jund and R. Jullien, Phys. Rev. Lett. **83**, 2210 (1999).
[41] National Research Council of the United States of America, *International Critical Tables* (McGraw–Hill, New York, 1926–1933).
[42] R. Brückner, J. Non-Cryst. Solids **5**, 123 (1970).
[43] D. L. Price and J. M. Carpenter, J. Non-Cryst. Solids **92**, 153 (1987).
[44] C. Meada, R. J. Hemley, and H. K. Mao, Phys. Rev. Lett. **69**, 1387 (1992).
[45] J. R. Horbach and W. Kob, Phys. Rev. B **60**, 3169 (1999).
[46] J. R. Horbach and W. Kob, Phys. Rev. E **64**, 041503 (2001).
[47] M. Wilson and P. A. Madden, Phys. Rev. Lett. **80**, 532 (1998).
[48] I. Okada, J. Mol. Liq. **83**, 5 (1999).
[49] M. C. C. Ribeiro, J. Phys. Chem. B **107**, 4392 (2003).